

# Physical modeling and analysis of P-wave attenuation anisotropy in TI media

Yaping Zhu, Ilya Tsvankin, and Pawan Dewangan, Center for Wave Phenomena, Department of Geophysics, Colorado School of Mines, Golden, CO 80401-1887, USA

## Summary

The amplitudes and frequency content of seismic waves propagating through anisotropic formations may be strongly distorted by directionally dependent attenuation. Here, we analyze physical-modeling measurements of the P-wave attenuation coefficient in a transversely isotropic (TI) phenolic sample.

Using the spectral-ratio method, we estimate the group (effective) attenuation coefficient of P-waves transmitted through the sample for a wide range of propagation angles (from  $0^\circ$  to  $90^\circ$ ) with the symmetry axis. Correction for the difference between the group and phase angles is used to obtain the normalized phase attenuation coefficient  $\mathcal{A}$ , which is then inverted for the Thomsen-style attenuation-anisotropy parameters  $\epsilon_Q$  and  $\delta_Q$ . Whereas the symmetry axes of the angle-dependent coefficient  $\mathcal{A}$  and of the velocity function have close orientations, the magnitude of the attenuation anisotropy far exceeds that of the velocity anisotropy. The quality factor  $Q$  increases more than tenfold from the symmetry (slow) direction to the isotropy plane (fast direction).

The robustness of our results depends critically on several factors, such as the availability of an accurate anisotropic velocity model and the adequacy of the “homogeneous” concept of wave propagation. The methodology discussed here can be extended to field measurements of anisotropic attenuation needed for AVO (amplitude variation with offset) analysis and seismic fracture detection.

## Introduction

Most existing publications on seismic anisotropy are devoted to the influence of angular velocity variation on the traveltimes and amplitudes of seismic waves. It is likely, however, that anisotropic formations are also characterized by directionally dependent attenuation related to the internal structure of the rock matrix or the presence of aligned fractures. Although experimental measurements of attenuation, both in the field and on rock samples, are relatively rare (e.g., Prasad and Nur, 2003), they indicate that attenuation anisotropy can be much stronger than velocity anisotropy. For example, according to the measurements of Hosten et al. (1987) for an orthorhombic sample made of composite material, the quality factor for P-waves changes from  $Q \approx 6$  in the vertical direction to  $Q \approx 35$  in the horizontal direction.

Here, we extend the spectral-ratio method to anisotropic media and apply it to P-wave transmission data acquired in a symmetry plane of a phenolic sample. Fitting the theoretical attenuation coefficient to the measurements

for a wide range of propagation angles yields large absolute values of the Thomsen-style attenuation-anisotropy parameters  $\epsilon_Q$  and  $\delta_Q$ .

## Theoretical background

### Attenuation in TI media

To facilitate the analytic description of TI attenuation, Zhu and Tsvankin (2004; hereafter, referred to as Paper I) developed a notation based on the same principle as the commonly used Thomsen parameters for velocity anisotropy. Under the assumption of “homogeneous” wave propagation, which means that the real ( $\mathbf{k}$ ) and imaginary ( $\mathbf{k}^I$ ) parts of the wave vector are parallel to each other, they studied the *normalized* attenuation coefficient defined as  $\mathcal{A} \equiv |\mathbf{k}^I|/|\mathbf{k}| = k^I/k$ . For P- and SV-waves, the set of Thomsen-style attenuation parameters includes the P- and S-wave attenuation coefficients in the symmetry direction,  $\mathcal{A}_{P0}$  and  $\mathcal{A}_{S0}$  (respectively), and the dimensionless anisotropy parameters  $\epsilon_Q$  and  $\delta_Q$ . The parameter  $\epsilon_Q$  determines the fractional difference between the normalized P-wave coefficients  $\mathcal{A}$  in the  $x_1$ - and  $x_3$ -directions, while  $\delta_Q$  governs P-wave attenuation for near-vertical propagation. In the limit of small attenuation and weak anisotropy (for both velocity and attenuation), the P-wave attenuation coefficient linearized in the anisotropy parameters has the form (Paper I)

$$\mathcal{A} = \mathcal{A}_{P0} (1 + \delta_Q \sin^2 \theta \cos^2 \theta + \epsilon_Q \sin^4 \theta), \quad (1)$$

where  $\theta$  is the phase angle with the symmetry axis.

### Spectral-ratio method for anisotropic media

For laboratory experiments, application of the spectral-ratio method typically involves amplitude measurements made under identical conditions for the sample of interest and for a reference purely elastic (non-attenuative) sample. The frequency-domain displacement of the direct wave recorded for the reference sample [superscript “(0)”] can be written as

$$U^{(0)}(\omega) = S(\omega) G^{(0)}(\mathbf{x}^{(0)}) e^{-\mathbf{k}_G^{(0)T} \cdot \mathbf{x}^{(0)}} e^{i(\omega t - \mathbf{k}_G^{(0)} \cdot \mathbf{x}^{(0)})}, \quad (2)$$

where  $\mathbf{x}$  is the vector connecting the source and receiver,  $S(\omega)$  is the spectrum of the source pulse,  $k_G^I$  is the amplitude decay factor (attenuation coefficient) in the group (ray) direction, and the factor  $G(\mathbf{x})$  incorporates the radiation pattern of the source and the geometrical spreading along the raypath. Similarly, the frequency-domain displacement for the attenuative sample [superscript “(1)”] has the form

$$U^{(1)}(\omega) = S(\omega) G^{(1)}(\mathbf{x}^{(1)}) e^{-\mathbf{k}_G^{(1)T} \cdot \mathbf{x}^{(1)}} e^{i(\omega t - \mathbf{k}_G^{(1)} \cdot \mathbf{x}^{(1)})}. \quad (3)$$

## P-wave attenuation in TI media

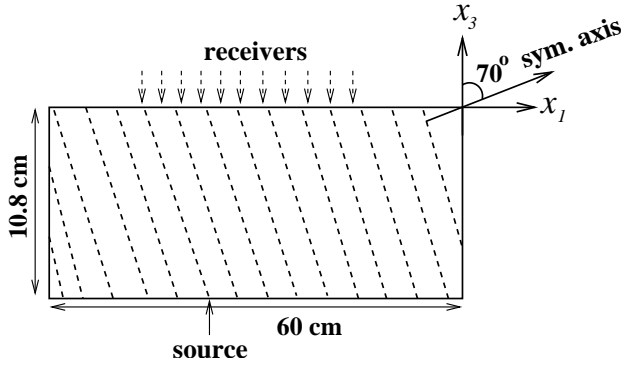


Fig. 1: Physical model of a TI layer with a tilted symmetry axis (TTI medium) prepared by Dewangan et al. (2005). The transmitted wavefield is excited by a transducer at the bottom of the model and recorded with a laser vibrometer. The measurements are made in the vertical plane that contains the symmetry axis (the *symmetry-axis* plane).

If the reference trace is acquired for a purely elastic medium with  $\mathbf{k}_G^{(0)I} = 0$ , the logarithm of the spectral amplitude ratio becomes

$$\ln \left| \frac{U^{(1)}}{U^{(0)}} \right| = \ln \left( \frac{G^{(1)}}{G^{(0)}} \right) - \mathbf{k}_G^{(1)I} \cdot \mathbf{x}^{(1)}. \quad (4)$$

We employ the following procedure of inverting P-wave attenuation measurements for the attenuation-anisotropy parameters. The slope of the logarithmic spectral ratio in equation (4) expressed as a function of  $\omega$  is used to estimate  $k_G^{(1)I}/\omega$ . (Under the assumption of frequency-independent  $Q$ ,  $k_G^{(1)I}$  is a linear function of  $\omega$ .) For homogeneous wave propagation in anisotropic media, the group and phase attenuation coefficients are related by  $k_G^I = k^I \cos(\psi - \theta)$ , where  $\psi$  and  $\theta$  are the group and phase angles, respectively (Paper I). Using the value of  $\theta$  computed from the known velocity parameters of the sample, we obtain the phase attenuation coefficient  $k^I$  from  $k_G^I$  and divide it by the corresponding real wavenumber  $k$  to estimate the normalized attenuation coefficient  $\mathcal{A} = k^I/k = (k^{(1)I}/\omega)V$ , where  $V$  is the phase velocity for the angle  $\theta$ . Finally, the measurements of  $\mathcal{A}$  for a wide range of phase angles  $\theta$  are inverted for the attenuation-anisotropy parameters  $\epsilon_Q$  and  $\delta_Q$ . Approximate values of  $\epsilon_Q$  and  $\delta_Q$  can be found from the linearized equation (1), but more accurate results are obtained by nonlinear inversion based on the exact Christoffel equation.

### Experimental setup

The goals of this experiment were to measure the directional dependence of the attenuation coefficient in a composite sample and to estimate the attenuation-anisotropy parameters. We used XX-paper-based phenolic material composed of thin layers of paper bonded with phenolic resin (Figure 1). This fine layering produces an effective anisotropic medium on the scale of the predominant wavelength.

The source and receivers were placed in the vertical symmetry plane of the sample, where wave propagation is described by the transversely isotropic model with a tilted symmetry axis (Dewangan et al., 2005). The P-wave source transducer was fixed at the bottom of the model, and the wavefield was recorded with a laser vibrometer moving at the layer's top with a sampling interval of 2 mm (Figure 1). The spread of the receiver locations was wide enough to record the full range of propagation angles (from  $0^\circ$  to  $90^\circ$ ) with respect to the symmetry axis.

For attenuation analysis we separated the first (direct) arrival by applying a Gaussian window to the raw data (Figure 2a). The amplitude spectrum of the windowed first arrival, obtained by filtering out the low ( $f < 5$  kHz) and high ( $f > 750$  kHz) frequencies, is shown in Figure 2b. An aluminum block with negligibly small attenuation served as the reference model. The spectrum of the reference trace recorded by a receiver located directly above the source was used to estimate the attenuation coefficient by means of the spectral-ratio method described above.

The parameters of the TTI velocity model needed to process the attenuation measurements were obtained by Dewangan et al. (2005) from reflection PP and PS data (Figure 3). P- and SV-wave propagation in TTI media is described by the P- and S-wave velocities in the symmetry direction ( $V_{P0}$  and  $V_{S0}$ , respectively), Thomsen anisotropy parameters  $\epsilon$  and  $\delta$ , and the angle  $\nu$  between the symmetry axis and the vertical. The known values of  $\nu = 70^\circ$  and of the thickness  $z = 10.8$  cm were accurately estimated from the reflection data, confirming the robustness of the velocity-inversion algorithm.

### Estimation of attenuation anisotropy

For each receiver position at the surface of the phenolic sample, we divided the spectrum of the windowed recorded trace by that of the reference trace, as suggested by equation (4). The relevant elements  $Q_{ij}$  of the quality-factor matrix are assumed to be constant in the frequency band (60–110 kHz) used in the analysis. The normalized phase attenuation coefficient  $\mathcal{A}$ , obtained after correcting for the difference between group and phase attenuation (it does not exceed 6%), exhibits a pronounced variation between the slow ( $0^\circ$ ) and fast ( $90^\circ$ ) directions (Figure 4). The largest attenuation coefficient is observed along the symmetry axis ( $\theta = 0^\circ$ ), where the P-wave phase velocity reaches its minimum value. Since the symmetry direction is orthogonal to the multiple thin layers bonded together to form the model, the rapid increase in attenuation toward  $\theta = 0^\circ$  is expected.

The polar plot of the attenuation coefficient, shown in Figure 5, indicates that the symmetry axis of the function  $\mathcal{A}(\theta)$  is close to that for the velocity measurements. To quantify the attenuation anisotropy, we estimated the best-fit Thomsen-style parameters from the exact Christoffel equation:  $\mathcal{A}_{P0} = 0.16$  ( $Q_{33} = 3.2$ ),  $\epsilon_Q = -0.92$ , and  $\delta_Q = -1.84$ . The linearized approximation (1) yields similar values ( $\mathcal{A}_{P0} = 0.16$ ,  $\epsilon_Q = -0.86$ ,

## P-wave attenuation in TI media

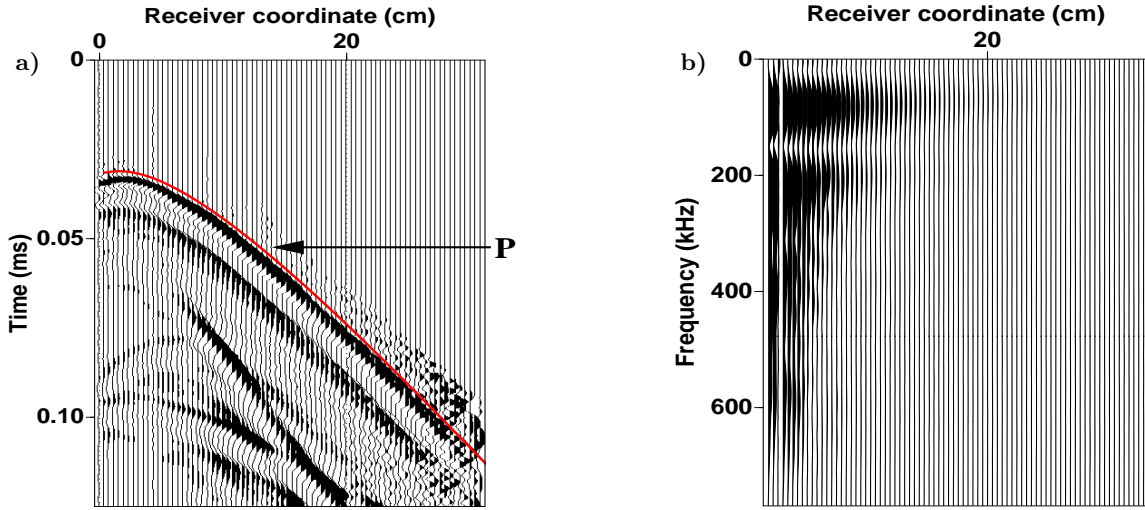


Fig. 2: (a) Raw transmission data excited by a P-wave transducer, and (b) the amplitude spectrum of the windowed first arrival. The solid line is the P-wave traveltimes modeled by Dewangan et al. (2005) using the inverted parameters from Figure 3. The time sampling interval is  $2 \mu\text{s}$ , and the width of the Gaussian window is 40 samples.

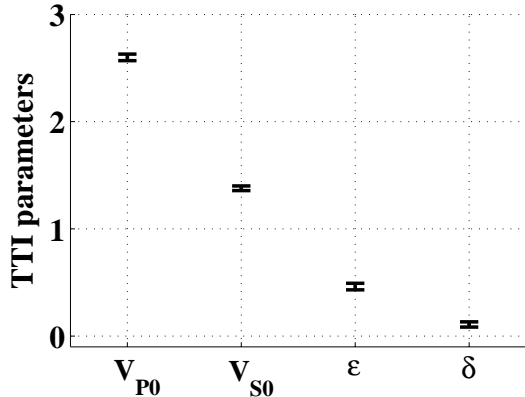


Fig. 3: Parameters of the TTI model estimated by Dewangan et al. (2005) from the reflection traveltimes of PP- and PS-waves in the symmetry-axis plane. The mean values are  $V_{P0} = 2.6 \text{ km/s}$ ,  $V_{S0} = 1.38 \text{ km/s}$ ,  $\epsilon = 0.46$ , and  $\delta = 0.11$ . The error bars mark the standard deviations in each parameter obtained by applying the inversion algorithm to 200 realizations of input reflection traveltimes contaminated by Gaussian noise. The standard deviation of the noise was equal to  $1/8$  of the dominant period of the reflection arrivals.

and  $\delta_Q = -1.91$ ) despite the significant angular variation of  $\mathcal{A}(\theta)$  (Figure 5). While the fact that the largest attenuation coefficient for this model is observed at the velocity minimum is predictable, the extremely low value of  $Q_{33} = 3.2$  is somewhat surprising. Note that estimates of the attenuation coefficient near the symmetry axis may be distorted by the relatively low reliability of amplitude measurements at long offsets corresponding to small  $\theta$  (Figure 1).

Problems in applying our methodology for large source-receiver distances may be related to such factors as the frequency-dependent geometrical spreading and the increased influence of heterogeneity. In general, the spectral-ratio method may not be adequate for describing the frequency spectrum of the long-offset data.

It is important to evaluate the uncertainty in the attenuation estimates caused by errors in the velocity-anisotropy parameters. Using the standard deviations in  $V_{P0}$ ,  $\epsilon$ ,  $\delta$ , and  $\nu$  provided by Dewangan et al. (2005), we repeated our inversion procedure for 50 realizations of the input TI velocity model (Figure 6). Although the variation of the estimated attenuation coefficients in some directions is not negligible, the mean values of the attenuation-anisotropy parameters obtained from the best-fit curve  $\mathcal{A}(\theta)$  are close to those listed above. The standard deviations are 2% for  $\mathcal{A}_{P0}$ , 0.01 for  $\epsilon_Q$ , and 0.06 for  $\delta_Q$ , which indicates that the influence of errors in the velocity field on our results is not significant. The attenuation-anisotropy parameters are somewhat more sensitive to moderate variations in the bounds of the frequency range used in the analysis.

## Discussion and conclusions

Since experimental measurements of attenuation are scarce, physical modeling of wave propagation through attenuative materials can provide valuable insights into the magnitude and angle variation of the attenuation coefficient. Here, we measured the P-wave attenuation coefficient and estimated the attenuation-anisotropy parameters for a transversely isotropic sample. Our results corroborate the conclusions of some previous experimental studies (e.g., Hosten et al., 1987; Prasad and Nur, 2003)

## P-wave attenuation in TI media

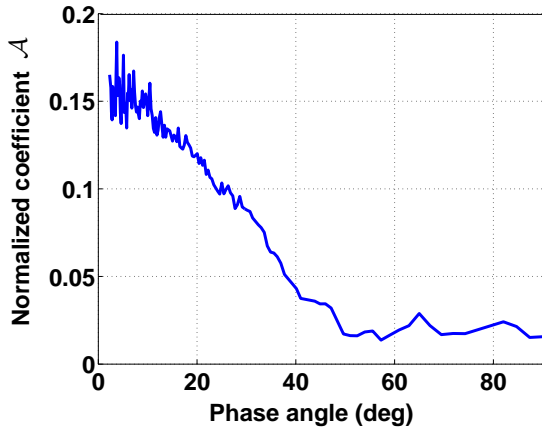


Fig. 4: Normalized P-wave attenuation coefficient  $\mathcal{A}(\theta)$  estimated from the data.

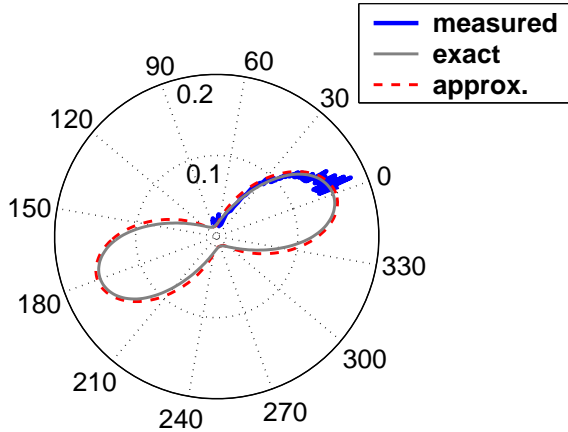


Fig. 5: Estimated attenuation coefficient from Figure 4 (black line) and the best-fit  $\mathcal{A}(\theta)$  obtained using the Christoffel equation (gray) and the approximate solution (1) (dashed).

that attenuation is often more sensitive to anisotropy than is either phase velocity or reflection coefficient.

While the large difference between the attenuation coefficients in the two principal directions is evident, the accuracy of our estimates strongly depends on several assumptions. First, our analytic solutions for the attenuation coefficient are based on the common assumption of homogeneous wave propagation (i.e., the real and imaginary parts of the wave vector are assumed to be parallel). For strongly attenuative models with pronounced anisotropy, this assumption may cause errors in the interpretation of attenuation measurements. Second, the radiation pattern of the source and geometrical spreading are taken to be frequency-independent in the frequency range used in the spectral-ratio method. Since the sample is heterogeneous, it is desirable to test the validity of this assumption, particularly for relatively large source-

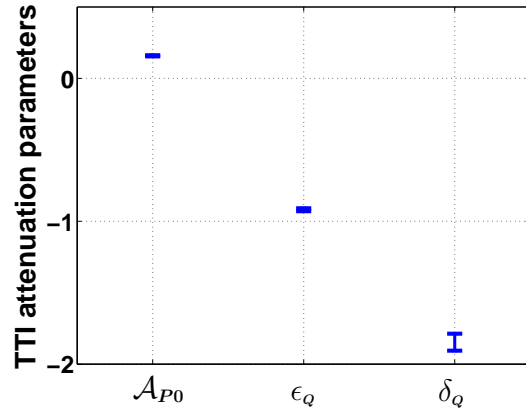


Fig. 6: Influence of errors in the velocity model on the attenuation parameters. The error bars mark the standard deviations in each parameter obtained by applying our algorithm with 50 realizations of the input TTI velocity parameters. The standard deviations in the velocity parameters are taken from Dewangan et al. (2005).

receiver offsets. Third, our data-processing sequence did not include compensation for the possible apparent attenuation related to the coupling coefficients at the source and receiver locations. Finally, estimation of the full set of Thomsen-style attenuation-anisotropy parameters requires combining P-waves with either shear data or converted PS-waves.

Although the experiment was performed using a laboratory sample, the results are indicative of the high potential of attenuation-anisotropy analysis for field seismic data.

## References

- Dewangan, P., Tsvankin, I., Batzle, M., van Wijk, K., and Haney, M., 2005, PS-wave moveout inversion for tilted transversely isotropic media: A physical-modeling study: 75th Ann. Internat. Mtg., Soc. Expl. Geophys., Expanded Abstracts.
- Hosten, B., Deschamps, M., and Tittmann B. R., 1987, Inhomogeneous wave generation and propagation in lossy anisotropic solids: application to the characterization of viscoelastic composite materials: Journal of the Acoustical Society of America, **82**, 1763–1770.
- Prasad, M., and Nur, A., 2003, Velocity and attenuation anisotropy in reservoir rocks: 73rd Ann. Internat. Mtg., Soc. Expl. Geophys., Expanded Abstracts, 1652–1655.
- Zhu, Y., and Tsvankin, I., 2004, Plane-wave propagation and radiation patterns in attenuative TI media: 74th Ann. Internat. Mtg., Soc. Expl. Geophys., Expanded Abstracts, 139–142.